JOURNAL OF GEOPHYSICAL RESEARCH VOLUME 65, NO. 3 MARCH 1960

A Theory of Trapping of Whistlers in Field-Aligned Columns of Enhanced Ionization[1]

R. L. SMITH AND R. A. HELLIWELL

Radio Propagation Laboratory
Stanford University
Stanford, California

AND

I. W. YABROFF

Stanford Research Institute
Menlo Park, California

Abstract. A ray theory of whistler propagation in ducts is developed for the purpose of explaining discrete whistler components. By use of refractive index surfaces and a Snell's law construction, it is shown that the only feature of the electron distribution affecting the trapping conditions is the ratio of the electron density in the column to that of the background. In most practical cases the electron density in the column required for trapping must be greater than the background level. Under certain conditions, however, the density in the column must be less than the background level. Using the theory, it is found that the enhancement required for trapping increases markedly toward the equator, providing a possible explanation for reduced whistler occurrence at the lower latitudes.

Introduction. *Storey* [1953] has shown that whistler energy travels approximately in the direction of the earth's magnetic field. The occasional occurrence of long echo trains with very low decrement led him to suggest in his doctoral dissertation that columns of auroral ionization, acting like wave guides, might prevent the spreading of energy, and thus account for the low decrement. Following the discovery of nose whistlers [*Helliwell and others,* 1956], this idea was extended to explain the discrete traces often exhibited in the spectrograms of whistlers. It was suggested that each trace resulted from the concentration of energy in a thin column of ionization acting as a duct and extending over a large part of the ionospheric path [*Helliwell,* 1956]. Further suggestions regarding the relationship of the discrete traces to ducts were made by *Storey* [1958]. Experimental evidence supporting the duct theory was obtained from an analysis of hybrid whistlers [*Helliwell,* 1959]. In this paper we shall develop a theory of the trapping of whistler energy in such ducts.

Although the existence of whistler ducts has not yet been directly verified, the idea seems reasonable on physical grounds. In regions of low collision frequency, the motion of charged particles is restricted to spiral orbits about the earth's magnetic field [*Alfvén,* 1950]. Irregularities of ionization density are thus constrained to diffuse primarily in the direction of the field, forming field-aligned columns. These columns will spread out in an east-west direction to form shells. An example is the thin shell of ionization produced in the Argus experiment [*Van Allen and others,* 1959].

Model. For simplicity of analysis, it is assumed that the properties of the duct change very slowly in the direction of the field lines. We can then represent the actual ionosphere with curved lines of force by a slab model in which the field is uniform and the ionization varies only in a direction normal to the field. The change in density is assumed to be very small in the space of a wavelength in the medium, so that ray theory will apply. The analysis also covers a model in which the ionization

[1] This paper was presented at a joint meeting of the URSI and IRE held in Washington, D. C., May 1959. The work was supported under Air Force contract AF 18(603)-126.

in the slab is constant over many wavelengths, then suddenly changes to a constant background level. The propagation of waves in such a sharply bounded model was discussed from the wave-theory viewpoint by *Northover* [1958] in a talk given at the 1958 joint fall meeting of URSI and IRE in Pennsylvania.

Method of ray tracing using refractive index surfaces. The ray tracing will be confined to a plane containing the magnetic field lines and the gradient of ionization. This choice is made because, as Storey has shown, the high refractive index for the whistler mode causes the ray path to be confined to the magnetic meridian. In our slab model the surfaces of constant refractive index are planes parallel to one another. Therefore the product of refractive index and the sine of the angle of incidence is a constant (simple form of Snell's law). It must be remembered, however, that the refractive index is a function of wave normal angle.

We will assume that the losses in the medium can be neglected, so that the ray direction describes unambiguously the direction of energy flow [*Hines*, 1951]. The ray direction is, in general, different from the wave normal direction in an anisotropic medium. It can easily be determined geometrically as shown, for example, by *Poeverlein* [1948]. A refractive index surface is constructed in spherical coordinates. The polar angle represents the wave normal direction, and the length of the radius vector to the surface represents the magnitude of the corresponding refractive index. We will call this radius vector the refractive index vector. For each wave normal direction, the ray direction is given by the perpendicular to the refractive index surface at the point where the refractive index vector intersects that surface. Brandstatter and Yabroff (private communication) have shown that the angle between the wave normal and ray direction must always be less that 90°. The ray velocity, not to be confused with the group ray velocity, is the wave velocity divided by the cosine of the angle between the ray and wave directions.

The refractive index surfaces can be used to determine the direction of reflected and transmitted waves at a sharp boundary. Consider the case of two homogeneous media separated by a plane boundary, as illustrated in Figure 1. A ray in direction ψ_1 with corresponding wave normal direction θ_1 is traveling in medium I toward the boundary. The normal to the boundary is $\bar{n}$ as shown. The direction of the transmitted and reflected rays can be determined geometrically by a Snell's law construction as follows. Superimpose the refractive index surfaces of media I and II on the same coordinate center and with the same reference direction. From the center of the coordinates a line is drawn in the incident wave normal direction θ_1 to intersect refractive index surface I at point P_1. A line is drawn parallel to $\bar{n}$ through P_1. The intersections with the refractive index surfaces represent possible transmitted and reflected waves. Note

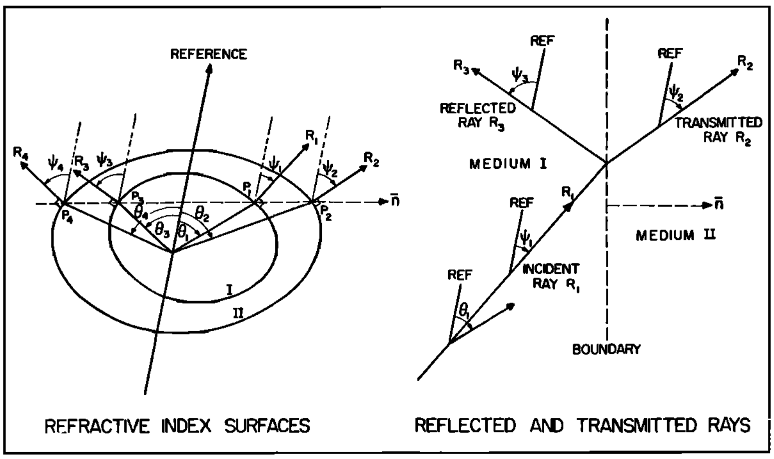

Fig. 1. Reflected and transmitted waves at a sharp boundary between two anistropic media.

that the tangential components of the refractive index of the incident, reflected, and transmitted waves are necessarily the same by this construction.

Not all the intersections necessarily represent propagating waves. In Figure 1, the intersection P_4 apparently represents a wave in medium II with energy traveling toward medium I. However, this particular wave does not exist, because it is not excited. Depending on the initial conditions and the nature of the refractive index, there may be none, one, or more transmitted or reflected waves.

The above construction can be extended to determine the differential refraction in a continuous medium where the resulting refracted waves are examined only in the neighborhood of the incident wave normal direction. However, $\bar{n}$, the normal to the boundary, is now taken to mean the direction of the space gradient of refractive index which is calculated holding the wave normal direction constant. The derivation of the above geometrical method was developed by Brandstatter and Yabroff from the work of Haselgrove. The differential equations for ray tracing are given by *Haselgrove* [1954].

Whistler refractive index surfaces. From the magneto-ionic theory [*Ratcliffe*, 1959], the refractive index surfaces which apply to whistler propagation can readily be computed. Assume that losses can be neglected and that the square of the plasma frequency is much greater than the product of wave frequency and gyrofrequency. Also assume that the wave frequency is less than the gyrofrequency. The wave refractive index is then given by [*Helliwell*, 1956]

$$\mu = f_0/[f_H\lambda^{1/2} (\cos\theta - \lambda)^{1/2}] \qquad (1)$$

where

f_0 = plasma frequency $\cong (80.6N)^{1/2}$.
N = electron density (number per cubic meter).
f_H = gyrofrequency.
λ = normalized frequency = f/f_H.
f = wave frequency.
θ = wave normal angle with respect to the magnetic field.

Note that the magnitude of the refractive index is directly proportional to the square root of electron density. The general shapes of the cross sections of refractive index surfaces computed from equation 1 are shown in Figure 2 for different ranges of the normalized frequency. Figure 2*a* shows the limiting shape of the refractive index surface as $\lambda \rightarrow 0$. This corresponds to the simplified formula for refractive index used by Eckersley and Storey. The ray direction is parallel to the magnetic field H only at $\theta = 0°$. Figure 2*b* shows the form of the refractive index surfaces for $0 < \lambda < 0.5$. The limiting cone for the refractive index surface is given by $\theta = \arccos\lambda$. For θ larger than this value, the refractive index is imaginary. The ray is parallel to the magnetic field at the angles $\theta = 0°$ and $\theta = \arccos(2\lambda)$. Figure 2*c* shows the form of refractive index surfaces for $0.5 < \lambda < 1$. The ray direction is parallel to the magnetic field only at $\theta = 0°$. The limiting cone is again given by $\theta = \arccos\lambda$.

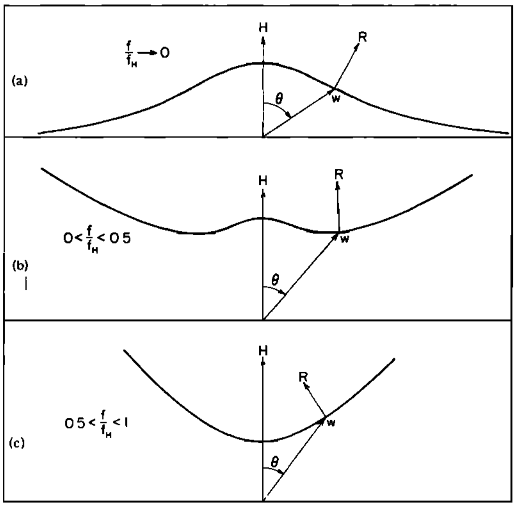

Fig. 2. Whistler refractive index surfaces.

An unusual example of ray behavior. Note that the effect of the anistropy may be so large as to cause the ray to turn away from regions of high refractive index, contrary to what is expected in the ray optics of an isotropic medium. This point requires some interpretation. Consider Figure 3, which shows the rays associated with a boundary separating two homogeneous media, and the related refractive index surfaces for a normalized frequency between 0.5 and 1. This boundary and

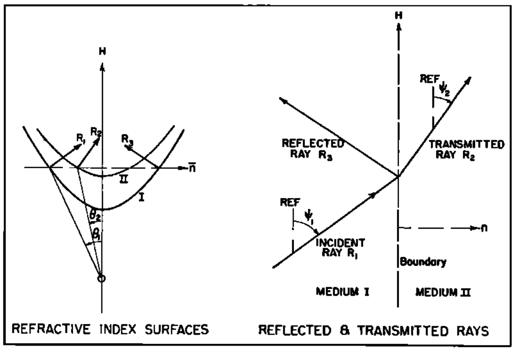

Fig. 3. Reflected and transmitted waves at a sharp boundary for $0.5 < \lambda < 1$.

the plane of incidence contain the direction of the static magnetic field H. Ray R_1 at angle ψ_1 in medium I is incident upon medium II. Its corresponding wave normal direction makes an angle θ_1 with respect to the reference direction (direction of H). For a given wave normal direction, the refractive index of medium I is less than that of medium II, as shown. The Snell's law construction gives the transmitted ray at angle ψ_2 with associated wave normal angle θ_2. Note that ψ_1 is less than ψ_2. Note further that the magnitude of the refractive index in medium II at angle θ_2 is less than the refractive index in medium I at angle θ_1. The wave normal angle rotates in the clockwise direction, as would be expected, when it enters a medium of higher refractive index. The ray direction, however, rotates in the opposite sense. There is no transmitted ray for incident wave normal angles less than a critical angle θ_c given by

$$\mu_1(\theta_c) \cos \theta_c = \mu_2(0)$$

This surprising behavior of the ray, obtained in a simple manner from the Snell's law construction, is not easily obtained by other methods.

Trapping conditions. The general nature of a ray path in a slab can be sketched as shown in Figure 4. The wave normal behavior is also shown. We take here the case of $\lambda = 0$, so that the refractive index surface shown in Figure 2*a* applies. Assume that the ray is started at a point on the line of maximum ionization with initial wave normal angle θ_0. The wave normal direction always rotates in the direction of increasing ionization. The correct direction of wave normal change can be determined from the Snell's law construction. This construction also defines the refractive index for each wave normal direction and hence the displacement of the ray path from a reference line x taken at the center of the slab in the plane of maximum ionization and parallel to H. The resulting ray path is similar to that shown at the right in Figure 4. After the ray crosses the axis of the slab, the behavior pattern is repeated, as shown in Figure 5*A*.

The ray direction is parallel to the magnetic field at the outermost excursion of the ray path. For this example, the ray is parallel to the magnetic field only when the corresponding wave normal angle is zero. We can now easily solve for the reduction in ionization density necessary to trap the ray in the slab.

Let $N(0)$ = electron density at the x axis.
$N(P)$ = electron density where the ray is parallel to the field, corresponding to the maximum excursion of the ray.

Since, by symmetry, the space gradient of refractive index is normal to the direction of H, the component of the refractive index vector along H must remain constant. Hence

$$\mu[N(0), \theta_0] = \mu[N(P), 0] \tag{2}$$

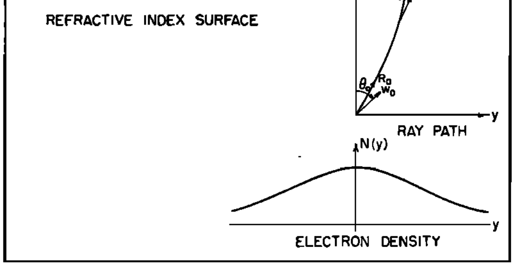

Fig. 4 Ray tracing in an enhancement of ionization aligned with the magnetic field.

With the approximation $\lambda << \cos\theta$, equation 1 is substituted in equation 2, giving

$$\left[\frac{N(0)}{\lambda\cos\theta_0}\right]^{1/2}\frac{\cos\theta_0}{f_H} = \left[\frac{N(P)}{\lambda}\right]^{1/2}\frac{1}{f_H} \quad (3)$$

$$\frac{N(P)}{N(0)} = \cos\theta_0 \quad (4)$$

The condition for trapping for this case is the same whether the refractive index changes very slowly or very rapidly compared with a wavelength. This result can be demonstrated by applying the Snell's law construction to a sharp boundary. It may be deduced that only the percentage change in ionization, not the gradient, is important in determining the trapping conditions. If the ray in the above case were started in an ionization minimum, or trough, the ray would bend away from the trough and not be trapped.

The case of $0 < \lambda < 0.5$ is more interesting. Consider first a ray starting at an ionization maximum, or crest, with an initial wave normal angle less than $\theta_2 = \text{arc}\cos(2\lambda)$. The ray will again be trapped if the ionization change is sufficient. Equations 3 and 4 are now modified to

$$\left[\frac{N(0)}{\lambda(\cos\theta_0 - \lambda)}\right]^{1/2}\frac{\cos\theta_0}{f_H} = \left[\frac{N(P)}{\lambda(1-\lambda)}\right]^{1/2}\frac{1}{f_H} \quad (5)$$

$$\frac{N(P)}{N(0)} = \frac{1-\lambda}{\cos\theta_0 - \lambda}\cos^2\theta_0 \quad (6)$$

It can be shown, again using the Snell's law construction, that the trapping condition given by equation 6 does not hold if the slab has a sharp boundary. We would expect, however, that the transmission coefficient would be fairly small if the ratio of ionization outside the slab to that inside the slab were less than that given by equation 6. Moreover, there is no reason to expect sharp boundaries in the outer ionosphere at whistler wavelengths, especially at the higher frequencies.

We will now consider the conditions for trapping in an ionization trough. If the initial wave normal angle, θ_0, is less than θ_3, given by solving

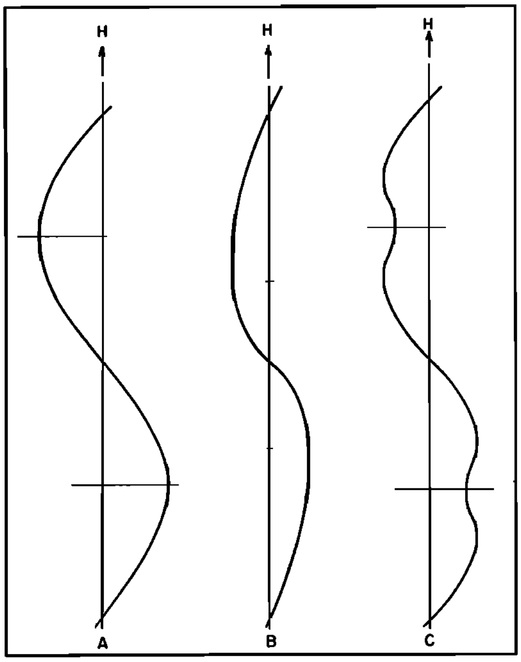

Fig. 5. Typical ray paths of trapped whistler energy.

$$\mu(\theta_3)\cos\theta_3 = \mu(0) \quad (7)$$

and if the ionization change is sufficient, the ray path will be similar to that shown in Figure 5*B*. If θ_0 is greater than θ_3, the ray path will be similar to that shown in Figure 5*C*. The above conclusions may be deduced using the Snell's law diagram.

The outermost excursion of the ray occurs in the above two cases at $\cos\theta_2 = 2\lambda$. This corresponds to the point on the refractive index surface where $\mu\cos\theta$ is a minimum. The condition for the minimum ionization change necessary for trapping then becomes

$$\left[\frac{N(0)}{\lambda(\cos\theta_0 - \lambda)}\right]^{1/2}\frac{\cos\theta_0}{f_H} = \left[\frac{N(P)}{\lambda^2}\right]^{1/2}\frac{2\lambda}{f_H} \quad (8)$$

$$\frac{N(P)}{N(0)} = \frac{\cos^2\theta_0}{4\lambda(\cos\theta_0 - \lambda)} \quad (9)$$

The above trapping condition also holds for the sharply bounded slab. For $\theta > \theta_2$, trapping can take place only in an ionization minimum or trough.

If $0.5 < \lambda < 1$, trapping likewise can take place only in a trough. The ray path will, however, be similar to that of Figure 5*A*. The trapping condition is the same as that given by equation 6. The same trapping condition holds for a sharply bounded slab.

The above results are summarized in Table 1 and are illustrated in a diagram of ray-path regions, shown in Figure 6. The ordinate is the cosine of the initial wave normal angle at the center of the slab, and the abscissa is the normalized frequency. The region outside the large triangle corresponds to imaginary values of refractive index. The lines separating the regions are defined in terms of θ through θ_4 given by:

$$\cos\theta_1 = \left(\frac{\lambda}{1-\lambda}\right)^{1/2} - \left[\frac{\lambda}{1-\lambda} - 2\lambda\left(\frac{\lambda}{1-\lambda}\right)^{1/2}\right]^{1/2}$$

$$\cos\theta_2 = 2\lambda$$

$$\cos\theta_3 = \lambda/(1-\lambda)$$

$$\cos\theta_4 = \lambda$$

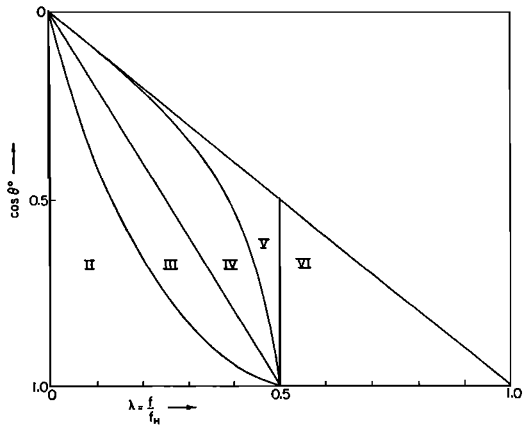

Fig. 6. Ray-path regions for trapped whistlers.

To each point in the triangle there corresponds a minimum change in ionization, or enhancement factor, necessary for trapping. In regions where trapping may take place in both troughs and crests, there are two values of this minimum change for each point. If the trapping occurs in a crest, we will define the enhancement factor to be

$$E_C = \frac{N(0)}{N(P)} - 1 \tag{10}$$

TABLE 1. Ray-Path Regions

Region	Defining Conditions	Type of Trapping Ionization	Equations for Enhancement	Typical Ray Path in Figure	Apply to Sharp Boundary?	Other Notes
I	$\lambda = 0$	Crest	4, 10	5*A*	Yes	
II	$0 < \lambda < 0.5$	Crest	6, 10	5*A*	No	$E_C < E_T$
	$0 \leq \theta_0 < \theta_1$	Trough	9, 11	5*B*	Yes	
III	$0 < \lambda < 0.5$	Crest	6, 10	5*A*	No	$E_T < E_C$
	$\theta_1 < \theta_0 < \theta_2$	Trough	9, 11	5*B*	Yes	
IV	$0 < \lambda < 0.5$, $\theta_2 < \theta_0 < \theta_3$	Trough	9, 11	5*C*	Yes	
V	$0.5 < \lambda < 1$, $\theta_0 < \theta_4$	Trough	6, 11	5*A*	Yes	

If the trapping occurs in a trough, we will define the enhancement factor to be

$$E_T = \frac{N(P)}{N(0)} - 1 \qquad (11)$$

Figure 7 is a diagram of the ray-path regions with contours of constant E_G and E_T.

Limitations. It would be expected that the use of the simple model presented here would be limited when applied to whistler propagation in the actual outer ionosphere. Obvious limitations are the geometrical factors of curvature and divergence of the earth's field lines, which cause the ducts to curve and vary in width. If the thickness of the ducts is more than a few hundred kilometers at the base of the ionosphere, i.e., comparable to the dimensions of the earth, then it would be necessary to use more advanced ray-tracing techniques, such as that employed by *Yabroff* [1958], to obtain more precise answers.

The use of our slab model also requires the variation of refractive index along the magnetic field to be small compared with the variations across the field, so that the gradient of refractive index is always normal to the field. We note here that both the gyrofrequency and the electron density above the *F*-layer maximum are expected to decrease with distance from the earth, and hence there is a tendency for the refractive index to remain constant. Indeed, for the model of the outer ionosphere, N proportional to f_H, as proposed by *Gallet* [1959] and others, and for $\lambda \rightarrow 0$, the refractive index remains constant along a given field line.

The restrictions of ray theory place a lower limit on the size of the ducts that can be analyzed by our theory. The ducts should be larger than a wavelength in the medium. However, the high refractive index for the whistler mode causes the wavelengths for a given frequency to be much smaller than the free-space value. Consider a medium, believed to be typical for whistler propagation, with a plasma frequency of 140 kc/s and a gyrofrequency of 50 kc/s. The wavelength of a 4 kc/s wave in this medium is 7.5 km. Field-aligned irregularities with dimensions less than a wavelength might guide the energy in a manner suggested by *Goubou* [1950]. The ducts here are not analogous to metallic wave guides, because the propagation conditions are similar both inside and outside the ducts.

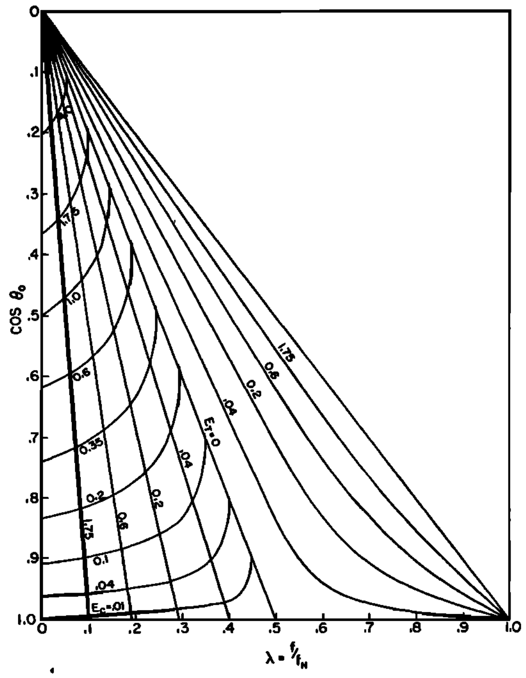

Fig. 7. Enhancement factors on the ray-path-region diagram.

Let us now consider the application of the theory to other models of the duct. The theory in its present form also applies where the ray tracing and the gradients of refractive index are confined to a plane. An example is the trapping of energy in an enhanced column of circular cross section if the initial excitation is given at a point on the axis of the column. This trapping theory can be extended to the more general three-dimensional case. The net results should not differ widely from those presented here if the direction of the gradient does not depart appreciably from the plane of the ray path.

Application to whistler propagation. As an application of the trapping theory developed above, let us now consider the effectiveness of a given duct as a function of geomagnetic latitude. As the whistler waves enter the ionosphere their wave normals are refracted to the vertical because of the high refractive index [*Storey*, 1953]. Thus the angle between the earth's field direction and the wave normal will increase toward the equator because of the decrease in the dip of the earth's field. One would expect, therefore, that the enhancement required for trapping would increase toward the equator. This idea has also been discussed qualitatively by *Storey* [1958].

The initial wave normal angle ϕ is then approximately equal to the complement of the magnetic dip and therefore can be expressed in terms of geomagnetic latitude l by

$$\tan \phi = \tfrac{1}{2} \cot l$$

We will assume that the trapping action of a duct begins in the lower regions of the path where the local gyrofrequency is much larger than the wave frequency. We can then use the approximation $\lambda \to 0$. Application of equation 4 then yields the desired minimum enhancement factor, which is plotted as a function of geomagnetic latitude in Figure 8. The required enhancements are seen to decrease markedly with increasing latitude.

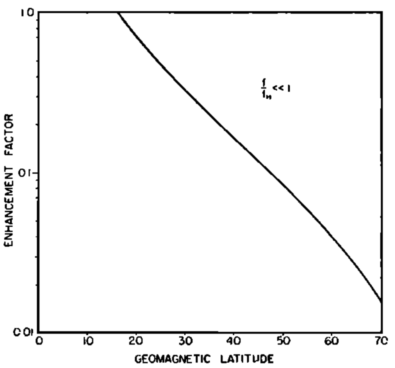

Fig. 8. Minimum enhancement factors for trapping as a function of geomagnetic latitude.

Since large enhancements would be expected to occur less frequently than small enhancements, Figure 8 predicts that whistler occurrence rate should increase with geomagnetic latitude. IGY data show that whistler rate does increase with latitude up to about 55°, then decreases. The decrease in rate above 55° can be attributed to decreasing thunderstorm activity at high latitudes, to a rapidly increasing path length, and to the rapid decrease in minimum gyrofrequency with increasing latitude. The attenuation increases very rapidly as the gyrofrequency approaches the wave frequency [*Helliwell,* 1956], and hence the number of whistlers observed in the usual frequency range would be expected eventually to decrease.

It has been noticed in the study of whistler echoes that the expected echoes of the leading components of one-hop whistlers are sometimes absent in the echo structure, although echoes of weaker components showing greater time delay are often present. Since the latter components are believed to represent whistlers traveling in ducts at higher latitudes, the explanation may be simply that a more favorable trapping angle is encountered upon reflection.

Further applications of the trapping theory are being studied, and will be presented at a later date. They include time-delay focusing effects due to the ducting, and high-frequency cutoff phenomena.

Conclusions. The main conclusions of this paper are:

1. The qualitative idea that whistler energy can be trapped in ducts is strongly supported by the theory presented, and the necessary conditions for trapping have been deduced.
2. Enhancement factors of about 10 per cent are required to trap whistlers in ducts at medium latitudes, and even less at higher latitudes.
3. The theory explains part of the variation of whistler rate with latitude.
4. A simple graphical method of analysis, the Snell's law construction, has been applied to obtain the results. We believe that this construction deserves wider use; its outstanding feature is that the ray behavior is easily seen on the same diagram with the wave normal behavior.

Acknowledgment. Helpful comments by L. A. Manning are acknowledged.

References

Alfvén, H., *Cosmical Electrodynamics,* Oxford University Press, 1950.

Gallet, R. M., The very low-frequency emissions generated in the earth's exosphere, *Proc. IRE, 47,* 211, 1959.

Goubou, G., Surface waves and their application to transmission lines, *J. Appl. Phys., 21,* 1119, 1950.

Haselgrove, J., Ray theory and a new method of

ray tracing, *Report of Physical Society Conference on Physics of the Ionosphere*, Cambridge, pp. 355–364, September 1954.
Helliwell, R. A., Low frequency propagation studies, part I: Whistlers and related phenomena: Final Report, Contract AF 19 (604)795, June 15, 1953, to Sept. 30, 1956 (revised, May 28, 1958), AFCRC-TR-56-189, ASTIA Document AD 110184, 1956.
Helliwell, R. A., Hybrid whistlers (Abstr.), Program of the joint meeting of URSI and IRE, Washington, D. C., p. 28, May 1959.
Helliwell, R. A., J. H. Crary, J. H. Pope,, R. L. Smith, The 'nose' whistler—a new high latitude phenomenon, *J. Geophys. Research, 61,* 139–142, 1956.
Hines, C. O., Wave packets, the Poynting vector, and energy flow, 4 parts, *J. Geophys. Research, 56,* nos. 1, 2, 4, 1951.
Northover, F. H., Propagation of electromagnetic waves along a columnar ionic irregularity (Abstr.), Program of the Joint meeting of URSI and IRE, Pennsylvania, p. 17, October 1958.
Poeverlein, H., Strahlwege von Radiowellen in der Ionosphäre, *Sitzber. bayer. Akad. Wiss.*, 1948.
Ratcliffe, J. A., *The Magneto-ionic Theory and Its Application to the Ionosphere,* Cambridge University Press, 1959.
Storey, L. R. O., An investigation of whistling atmospherics, *Phil. Trans. Roy. Soc. London, Ser. A, 246,* 113–141, 1953.
Storey, L. R. O., A method to interpret the dispersion curves of whistlers, D. R. T. E., Ottawa, RPL, no. 23-41, April 1958.
Van Allen, J. A., Carl E. McIllwain, and George H. Ludwig, Satellite observations of electrons artificially injected into the geomagnetic field, *J. Geophys. Research,* 64, 877–891, 1959.
Yabroff, I. W., Whistler paths in the outer ionosphere (Abstr.), Program of the joint meeting of the URSI and IRE, Washington, D. C., p. 41, April 23–26, 1958.

(Manuscript received December 3, 1959.)